Proc. Natl. Acad. Sci. USA
Vol. 83, pp. 9488–9492, December 1986
Cell Biology

Fluid phase endocytosis by cultured rat hepatocytes and perfused rat liver: Implications for plasma membrane turnover and vesicular trafficking of fluid phase markers

(bile/bile acid/microtubules/transcytosis/vesicle)

BRUCE F. SCHARSCHMIDT*, JOHN R. LAKE, EBERHARD L. RENNER, VOJTECH LICKO, AND REBECCA W. VAN DYKE

Department of Medicine and Liver Center, University of California, San Francisco, CA 94143

Communicated by Rudi Schmid, August 22, 1986

ABSTRACT **Hepatocytes take up a variety of ligands via receptor-mediated endocytosis, yet little is known regarding either the volume of fluid or the amount of membrane internalized via endocytosis in liver cells. In these studies, we have utilized radiolabeled inulin to characterize fluid phase endocytosis by rat hepatocytes in primary culture and perfused rat liver. Uptake of inulin by cultured hepatocytes was nonlinear with time, occurring most rapidly during the first 2 min. Inulin uptake and efflux in cultured hepatocytes and inulin uptake by perfused rat liver were kinetically compatible with the entry of inulin into a rapidly ($t_{1/2}$, 1–2 min) turning-over (presumably endosomal) compartment that exchanged contents with the extracellular space and comprised ≈3% of hepatocyte volume, as well as entry into and concentration of inulin within slowly ($t_{1/2}$, >1 hr) turning-over storage compartments. Based on inulin uptake, it is estimated that cultured hepatocytes endocytosed the equivalent of 20% or more of their volume and 5 or more times their plasma membrane surface area each hour. Neither chloroquine (1 mM) nor taurocholate (200 μM) affected inulin handling by cultured cells, whereas colchicine (10 μM) inhibited transfer to storage compartments by >50%. In conjunction with our previous observations, the present findings suggest that inulin endocytosed across the basolateral membrane is largely (≈80%) regurgitated back into plasma, with smaller amounts transported to intracellular storage compartments (≈18%) or to bile (≈2%). Transport of inulin via these pathways is unaffected by taurocholate and does not require vesicle acidification, whereas intact microtubular function is required for transfer to storage compartments or biliary secretion.**

The ability to internalize extracellular material appears to be a property shared by most, if not all, cells. Hepatocytes are actively endocytic and internalize a variety of ligands by receptor-mediated endocytosis (1, 2), yet relatively little is known regarding the overall rate at which hepatocytes internalize extracellular fluid or fluid phase markers (3, 4).

We have recently reported evidence that the intact perfused rat liver transports a variety of fluid phase markers from perfusate to bile via a transcellular vesicular mechanism (5). In the present study, we have extended these observations in perfused liver and also characterized fluid phase endocytosis by rat hepatocytes in primary culture. In addition to measuring the rate at which hepatocytes endocytose extracellular fluid, our principal objectives were as follows. First, several recent reports indicate that fluid phase markers are internalized initially into a compartment that exchanges with extracellular fluid (6–8); however, the kinetics of this process, which presumably reflect membrane recycling, remain incompletely characterized. We therefore sought evidence of such a process in mammalian liver and characterized it kinetically. Our second objective was to integrate observations in perfused liver and cultured hepatocytes so as to develop a quantitative overview of pathways of fluid phase endocytosis by intact liver.

MATERIALS AND METHODS

Chemicals and Radioisotopes. Inulin (M_r, 5000), dextran (average M_r, 81,600), and all other chemicals were obtained from Sigma. [^{3}H]Inulin, [^{14}C]inulin, and 3-*O*-[*methyl*-^{14}C]-methyl-D-glucose were purchased from New England Nuclear. [^{3}H]Dextran (average M_r, 70,000) was obtained from Amersham.

Analytical and Preparative Techniques. [^{3}H]Dextran was separated from low molecular weight radiolabeled contaminants by column chromatography as described (5). Radiolabeled inulin was prepared similarly by column (1 × 40 cm) chromatography using Sephadex G-25; this same technique was used for analysis of radiolabeled inulin extracted from cells. Radioactivity was measured by liquid scintillation counting using internal or external standardization for quench correction. Samples of liver tissue were digested with Soluene 350 (Packard) and decolorized with H_2O_2/isopropanol prior to counting.

Cultured Hepatocytes. Rat hepatocytes (>98% pure), prepared as described (9–11), were plated on plastic dishes and maintained in modified 1990R medium supplemented with amino acids, insulin, and corticosteroids for 48 hr before use. Uptake studies were performed as described (9, 10). Briefly, following preincubation in an unsupplemented balanced electrolyte solution (10 min for most studies, 2 hr for studies with colchicine or lumicolchicine), cells were incubated for various times in medium identical to that used for the preincubation except for the presence of radiolabel. Time points were obtained at 10, 20, 30, and 40 sec, and at 1, 3, 5, 10, 15, 20, 30, 40, 60, and 120 min for all uptake studies. Cells were then washed free of extracellular radioisotope by dipping the culture plate for 10 sec in each of eight beakers containing 25 ml of ice-cold (4°C) incubation medium without isotope but with 10 mg of unlabeled dextran or inulin per ml. In both previous studies (9, 10) and preliminary studies (not presented), this technique was shown to satisfactorily remove extracellular ^{22}Na, ^{36}Cl, [^{3}H]taurocholate, [^{3}H]inulin, and [^{3}H]dextran, with <0.1% present in beakers 5–8. Cells were then scraped into 0.1 M NaOH/0.189 M Na_2CO_3, in which radioactivity and protein were measured. Intracellular volume was determined using radiolabeled 3-*O*-[*methyl*-^{14}C]-methyl-D-glucose (9, 10). For analysis of cell-associated radiolabel, 10 cell plates were scraped into 1.5 ml of phos-

The publication costs of this article were defrayed in part by page charge payment. This article must therefore be hereby marked "*advertisement*" in accordance with 18 U.S.C. §1734 solely to indicate this fact.

*To whom requests for reprints should be addressed.

phate-buffered saline containing 2% Triton X-100, and 200 μl of this solution was applied to the column (see above).

Efflux of radiolabeled inulin from cells was measured by preincubating each dish in medium containing radiolabeled inulin for 5 or 60 min and then washing the cells as described above. Warmed medium (37°C), free of radiolabel, was then added to each dish, and this isotope-free medium was completely replaced at frequent intervals up to 30 min. Radiolabel in each complete change was measured, as was residual radiolabel present in the cells at 30 min, and efflux was calculated as a percentage of the total radiolabel present in the cells at the end of the ice-cold wash. Companion studies were performed at 4°C, and the effects of perturbations on uptake were assessed by comparing concurrent control and experimental cells from the same cohort.

The mean diameter of the cultured hepatocytes was determined from projected light photomicrographs of the monolayer (total magnification, ×400). The largest and smallest transverse dimension was measured for each of 68 cells from 10 monolayers and five cell batches. Mean cell thickness was determined from transmission electron micrographs prepared as described (2).

Isolated Perfused Rat Liver. The surgical techniques, design, and operation of the fluorocarbon-perfused rat liver apparatus were as described (5). Following an initial equilibrium period of 30 min, [^{14}C]inulin was added to the perfusate along with 10 μM unlabeled inulin, and duplicate biopsy samples (45–220 mg each) were taken from the periphery of the liver lobes at 7, 15, 30, 60, and 90 min. Radioactivity in perfusate and liver tissue was measured as described above, and there was close agreement (mean difference of 7.6% ± 2.8%) between the paired specimens.

Mathematical Analyses. The data were analyzed by a nonlinear least-squares procedure. Sums of exponential functions were fitted to the uptake and efflux curves, and the best-fit function was determined to be the simplest (i.e., smallest number of parameters) function associated with the smallest sum of squares by *F* test. Models corresponding to the uptake and efflux functions are presented in the *Appendix*. The significance of differences between parameters computed for various experimental conditions was estimated using the Student's *t* test.

RESULTS

Inulin Uptake as a Measure of Fluid Phase Endocytosis. Inulin uptake within a single batch of cultured hepatocytes exhibited a mean coefficient of variation of 9.8%, but it varied as much as 2-fold between batches. Therefore, all experimental manipulations were compared with concurrent controls. Inulin uptake as a measure of fluid phase endocytosis by hepatocytes was validated by the following observations: (*i*) Uptake of inulin at 37°C and 4°C varied linearly (mean *r* value averaged 0.98) with extracellular inulin concentration (0.5–5.0 mg/ml) when measured at both 5 min and 60 min. (*ii*) The elution profile of radiolabeled inulin recovered from the cells after 1 hr was similar to that of inulin present in the medium. (*iii*) Uptake was decreased at 4°C as compared with 37°C (Fig. 1, Table 1). (*iv*) In four cell batches, uptake of inulin (10 sec to 120 min) averaged 0.96 ± 0.04 (mean ± SEM; $n = 79$) of concurrently measured uptake of dextran, which was also found to be nonsaturable over the concentration range of 1–10 mg/ml.

Cellular Volume and Cell Dimensions. Intracellular volume in seven hepatocyte cultures averaged 1.90 ± 0.18 μl/mg, similar to previous estimates (9, 10). Mean minimum and maximum transverse dimensions were 29 and 39 μm, respectively. Maximal cell thickness averaged 2 μm.

Characterization of Inulin Uptake Under Control Conditions (Fig. 1, Table 1, and *Appendix A*). Inulin uptake at 37°C was most rapid during the first 2 min and was followed by a slower steady rate of inulin accumulation to 120 min. This biphasic pattern was not the result of cell exhaustion, since an identical pattern of uptake was seen when radiolabel was added after a 1-hr preincubation in unlabeled inulin (not shown). Kinetic analysis of the uptake data at 37°C required a two-component function plus a constant term of the form

$$C(t) = P_1[1 - \exp(-P_2 t)] + P_3 t + P_4, \quad [1]$$

indicating the presence of at least two intracellular compartments as well as surface binding. The initial curvilinear phase of inulin uptake was represented by an exponential component with a $t_{1/2}$ (= ln 2/P_2) of 1–2 min and a steady-state value (P_1) corresponding to an apparent volume of 0.069 μg·mg^{-1}. The subsequent apparently slower rate of net inulin accumulation (0.0080 μg per mg of cell protein per min) was described

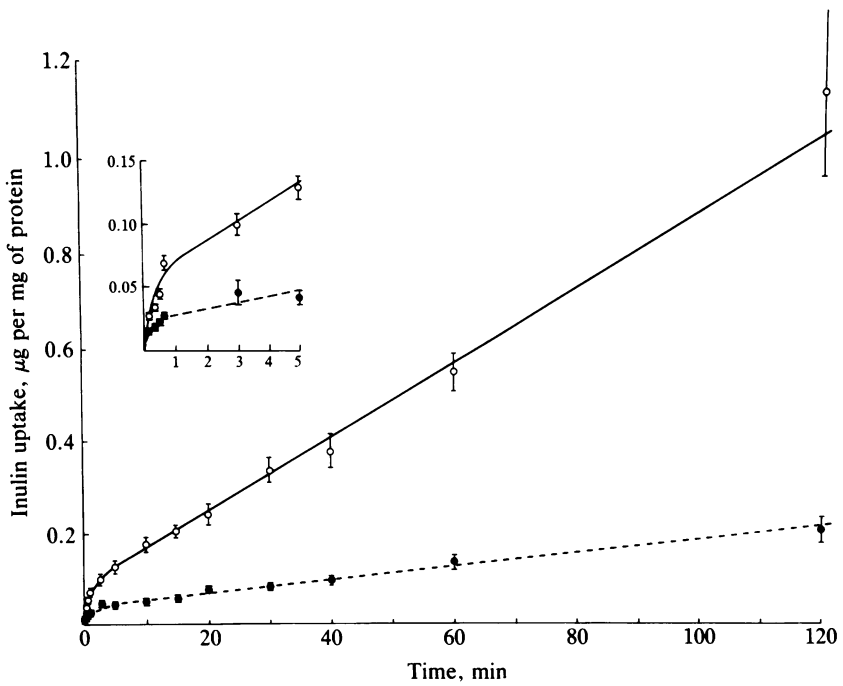

FIG. 1. Inulin uptake vs. time. (*Inset*) Early time points. Each 37°C data point (○) represents the mean ± SEM of triplicate determinations in each of 13–27 cell batches and includes control data points depicted separately in Figs. 2 and 3. Each 4°C (●) data point represents the mean ± SEM of triplicate determinations in 10–22 cell batches. The lines represent best fits of Function 1.

Table 1. Parameters of inulin uptake

	P_1, μg per mg of protein	P_2, min^{-1}	P_3, μg per mg of protein per min	P_4, μg per mg of protein
Control				
37°C*	0.069 ± 0.008	0.805 ± 0.213	0.0080 ± 0.0004	0.019 ± 0.004
4°C	0.023 ± 0.003†	0.913 ± 0.282	0.0015 ± 0.0001†	0.013 ± 0.002
Taurocholate (60 min)				
Control	0.077 ± 0.028	0.335 ± 0.219	0.0078 ± 0.0012	0.034 ± 0.005
Experimental	0.110 ± 0.020	0.837 ± 0.324	0.0086 ± 0.0012	0.018 ± 0.007
Chloroquine				
Control	0.052 ± 0.009	1.05 ± 0.409	0.0069 ± 0.0006	0.009 ± 0.004
Experimental	0.086 ± 0.022	0.596 ± 0.318	0.0096 ± 0.0012	0.016 ± 0.006
Colchicine				
Control (lumicolchicine)	0.139 ± 0.035	0.337 ± 0.168	0.0135 ± 0.0014	0.058 ± 0.008
Experimental	0.252 ± 0.033†	0.299 ± 0.081	0.0061 ± 0.0010†	0.035 ± 0.007

All uptake curves were measured at 37°C (except where indicated) at an extracellular inulin concentration of 1 mg/ml. Thus, uptake of 1 μg of inulin represents endocytosis of 1 μl of extracellular fluid. The function [1] describing uptake that incorporates these parameters is described in *Results*.

*This group represents all studies performed at 37°C (n = 13–27 for each time point) and includes controls (n = 4–6 for each time point) that were done concurrently with taurocholate and chloroquine incubations that are listed separately in the table.

†$P < 0.005$ compared with respective 37°C control group.

by a linear term (P_3), which, based on efflux data, likely represents an exponential component with a $T_{1/2}$ much longer than the duration of the study (see below). Apparent binding (P_4) represented 15% of total cell-associated inulin at 5 min under control conditions (range, 7–19%) for all uptake studies (Table 1). Initial inulin uptake rate at 37°C was 0.064 $\mu g \cdot mg^{-1} \cdot min^{-1}$, as computed from the derivative of this function at time zero ($P_1 \cdot P_2 + P_3$).

The curves describing inulin uptake at 4°C (Fig. 1, Table 1) and cold-sensitive inulin uptake (uptake at 4°C subtracted from that at 37°C; not shown) were also best described by Function 1. Initial inulin uptake rate, net inulin accumulation rate, and the apparent steady-state volume of the exponential component were decreased by 65–81% at 4°C as compared with 37°C, whereas the half-life of the exponential component was unchanged. Initial cold-sensitive inulin uptake rate and inulin accumulation rate were 0.0328 $\mu g \cdot mg^{-1} \cdot min^{-1}$ and 0.0059 $\mu g \cdot mg^{-1} \cdot min^{-1}$, respectively. Uptake at 4°C did not differ in the presence of taurocholate, chloroquine, lumicolchicine, or colchicine at any time point as compared with control incubations at 4°C; all 4°C data were therefore combined for Fig. 1.

Efflux of Radiolabeled Inulin (Fig. 2, Table 2, and *Appendix A*). Kinetic analysis of inulin efflux following a 5- or 60-min preincubation required a function with two exponential components of the form

$$C(t) = Q_1 \exp(-Q_2 t) + Q_3 \exp(-Q_4 t), \quad [2]$$

indicating the presence of two intracellular compartments, which exchanged directly or indirectly with the extracellular space. The estimated $t_{1/2}$ (= $\ln 2/Q_2$) of the early component of efflux was comparable to the estimate based on analysis of uptake (see above). Analyses (not shown) of cold-sensitive inulin efflux (efflux at 37°C minus efflux at 4°C for each time point) yielded values for the half-life and apparent size of the early component similar to those at 37°C. However, the apparent half-life of the second exponential component was increased from 1–2 hr to 4–6 hr. This is consistent with slow turnover of the storage compartments and may help to account for the apparently linear second component of the function describing uptake (see below). More precise estimates of the $t_{1/2}$ (= $\ln 2/Q_4$) of the slow component of efflux would require measurements of inulin uptake or efflux over much longer periods than in the present study.

Compatibility of Uptake and Efflux Data. If the data for inulin uptake and efflux represent the same linear transport processes, then the parameters calculated for function 1 should be compatible with the parameters for function 2. Because the function describing efflux dictates that both compartments exchange directly or indirectly with the extracellular space, the general function describing uptake should be of the form

$$C(t) = P_1[1 - \exp(P_2 t)] + P_3'[1 - \exp(-Q_4 t)] + P_4. \quad [3]$$

Function 3 is equivalent to Function 1 for all observation times (t) much less than the $t_{1/2}$ of the second component ($t << 1/Q_4$), where $P_3' = (P_3/Q_4)$ is a new parameter corresponding to the apparent size of the slow component of uptake at steady state. For any preloading time, it can be shown that efflux parameters of Function 2 (Q_1, Q_2, Q_3, and Q_4) can be computed from uptake parameters of Function 1, and as shown in Fig. 2, the observed efflux data (solid circles) fall along the curve (dashed line) predicted from efflux parameters computed from the uptake parameters of Function 1, indicating compatibility of the uptake and efflux functions.

Inulin Uptake by Perfused Rat Liver. In four perfusions,

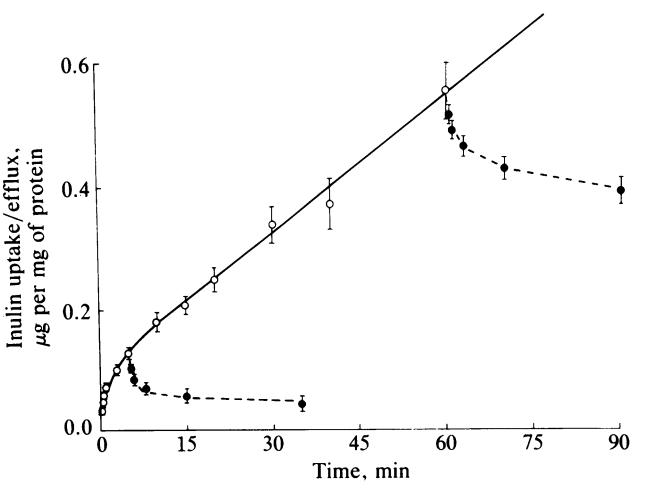

FIG. 2. Inulin uptake (○) and efflux (●) at 37°C vs. time. The uptake curve (solid line) is the same as that depicted in Fig. 1, whereas efflux was determined in cells preincubated for 5 or 60 min in radiolabeled inulin. Data points describing efflux represent the mean ± SEM of duplicate or triplicate determinations in each of four to six cell batches and fall close to a curve (dashed line) that was compatible with the uptake data as described in *Results*.

Table 2. Parameters of inulin efflux

	Q_1, % of total	Q_2, min^{-1}	Q_3, % of total	Q_4, min^{-1}
Preincubation (5 min)				
37°C	38.6 ± 2.3	0.835 ± 0.521	50.8 ± 4.74	0.015 ± 0.004
4°C	18.6 ± 4.5*	0.992 ± 0.446	81.4 ± 1.51*	0.006 ± 0.001
Preincubation (60 min)				
37°C	14.0 ± 2.6†	0.537 ± 0.251	79.5 ± 2.0†	0.005 ± 0.001
4°C	11.0 ± 2.1	0.582 ± 0.282	85.7 ± 1.5	0.003 ± 0.001

Efflux curves were measured at 37°C and 4°C following a 5-min or 60-min preincubation in inulin (1 mg/ml) as described in *Materials and Methods*. The function [2] describing efflux that incorporates these parameters is described in *Results*.
*$P < 0.05$ compared with 37°C.
†$P < 0.05$ compared with 5-min preincubation.

inulin uptake into perfused liver tissue was linear (mean r = 0.85) with time to 90 min, and represented a rate of fluid internalization of 0.764 ± 0.10 $\mu l \cdot min^{-1} \cdot g^{-1}$ liver tissue or, assuming 16% protein by weight for rat liver (12), 0.0048 ± 0.0006 $\mu l \cdot mg^{-1} \cdot min^{-1}$. This agrees surprisingly well with the apparent rate of fluid uptake by cultured cells either at 37°C (0.0080 $\mu l \cdot mg^{-1} \cdot min^{-1}$; Table 1) or when corrected for 4°C incubation (0.0059 $\mu l \cdot mg^{-1} \cdot min^{-1}$).

Effect of Taurocholate, Chloroquine, and Colchicine on Inulin Uptake (Fig. 3, Table 1). Taurocholate [200 μM, increases bile flow by perfused rat liver by >50% (5)] and chloroquine [1 mM, which alkalinizes acidic intracellular compartments identified using acridine orange in this same cultured hepatocyte system (13)] did not alter inulin handling by cultured hepatocytes (Table 1). Colchicine (10 μM), by contrast, as compared with lumicolchicine, decreased the rate of net inulin accumulation (P_3, Function 1) by ≈55% and increased the steady-state value of the initial exponential component (presumably representing an increase in the apparent size of the rapidly turning-over pool), but it had no significant effect on the initial rate of inulin uptake. Similarly, in perfused liver, neither taurocholate nor chloroquine altered the biliary secretion of fluid phase markers (5, 14), whereas colchicine decreased the vesicular transport of fluid phase markers from perfusate to bile by 60–80% (5, 14, 15).

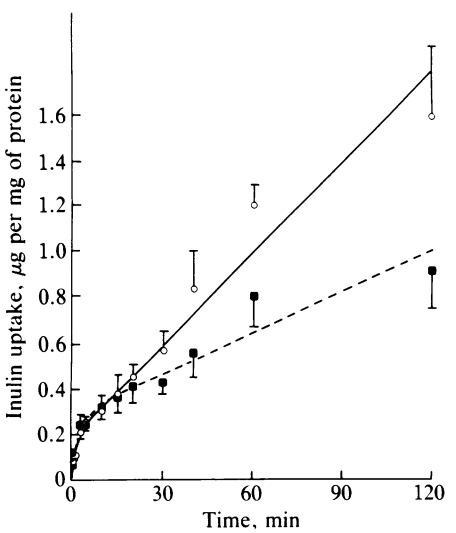

FIG. 3. Inulin uptake at 37°C in the presence of lumicolchicine (○) or colchicine (■) (10 μM). Each data point represents the mean ± SEM of duplicate or triplicate determinations in each of four to six cell batches. The curves represent best fits of Function 1 (Table 1). Uptake at 4°C in the presence or absence of colchicine did not differ from that depicted in Fig. 1 and is not shown.

DISCUSSION

The present studies confirm previous observations in other cell types, which suggest that internalized marker first enters a compartment that rapidly exchanges its contents with plasma (6–8, 16), and permit a more precise estimate of the kinetics of this process than has previously been possible. The estimated $t_{1/2}$ of 1–2 min for recycling of fluid phase markers is shorter than previous estimates of 5 min (alveolar macrophages), 6–8 min (fibroblasts), 15 min (L cells), or 20 min (adipocytes) based on comparatively few early time points (1, 6–8), but it is similar to the estimated half-life for the chloroquine-insensitive retroendocytosis or diacytosis of intact receptor–ligand complexes (1, 17). While neither our observations nor the previous observations of others exclude the possibility that the early component of the uptake curve (Fig. 1) represents cold-sensitive binding rather than uptake, this seems unlikely in light of the wash procedure used, the good correspondence between estimates of the early component derived from uptake and efflux studies (Tables 1 and 2), and the good agreement between results with inulin and dextran.

The present studies also provide information regarding the rate of internalization, and hence turnover, of the hepatocyte plasma membrane via endocytosis. Modeling the intact cultured hepatocyte as a cylinder 2 μm in height and 35 μm in diameter (see *Results*), the rate of cold-sensitive net inulin accumulation (P_3, Function 1) by hepatocytes represents a rate of fluid internalization equal to ≈20% of hepatocyte volume per hr, and, coupled with estimated average vesicular diameters of 50–200 nm (18), endocytosis of an area of membrane equivalent to 5–20 times the total surface of the hepatocyte every hour. This estimate increases still further if the corresponding rates are calculated from initial inulin entry rate. These estimated rates of membrane turnover are faster than those estimated for macrophages and L cells (up to 2 times per hour) and adipocytes (≈0.2 times per hour) (16, 18). This rapid rate of fluid internalization may also account for much of the nonsaturable uptake by hepatocytes of ligands such as transferrin-bound iron or low density lipoprotein (19).

Integration of our present and previous observations regarding rates of inulin uptake, sequestration, and biliary secretion in cultured hepatocytes and perfused rat liver, which appears justified given the similar rates of inulin accumulation and similar effects of taurocholate, chloroquine, and colchicine in the two models, also permits tentative conclusions regarding the pathways of fluid phase marker transport by liver cells. This analysis assumes that uptake and efflux occur across the basolateral membrane in cultured hepatocytes and that inulin accumulation by perfused liver represents uptake by hepatocytes. These assumptions rest on the observations that the basolateral membrane represents ≈87% of the hepatocyte cell surface, that canalicular space in cultured cells appears to exchange poorly with medium (20), and that the time course of perfused

liver studies is sufficient for distribution into the extracellular space and for steady-state biliary secretion to occur (5). Given these assumptions, the findings are consistent with a model (*Appendix A*) in which inulin is rapidly internalized into a compartment, presumably representing endosomes, which represents 3.3% of cell volume, similar to the estimate of 2.5% previously reported for macrophages using stereologic techniques (18). Of this internalized marker, most (≈80%) is rapidly regurgitated back into plasma across the basolateral membrane, with apparently smaller amounts transferred to intracellular storage compartments (≈18%), and secreted into bile (≈2%) (*Appendix B*). In contrast to the plausible estimates of endosomal volume, the unrealistically large estimate of the volume of storage compartments at 120 min (≥50% of cell volume; Function 3 and *Appendix A*) indicates that internalized marker is progressively concentrated concurrent with transfer to these storage compartments, which likely include prelysosomal compartments such as multivesicular bodies as well as lysosomes (13). While these estimates of fluid phase marker trafficking cannot be generalized to ligands, it is of interest that ≈2% of asialoglycoprotein, most of which is catabolized in lysosomes, is also transported intact to bile (14, 21).

Finally, our observations indicate that intact microtubular function is required for transfer of internalized marker to storage compartments or bile, but not for initial uptake into the early endosomal compartment. This is consistent with the observation in intact liver that colchicine appears to inhibit transport to bile, but not initial internalization, of immunoglobulin A (2, 15), and the apparent increase in the size of the endosomal pool following treatment with colchicine would be consistent with a role for microtubules in vesicle recycling. In contrast to colchicine, no effect of chloroquine on the sequestration or transport to bile of inulin or dextran was observed. Thus, while acidification of endosomal vesicles (22) may be required for normal receptor–ligand dissociation, lysosomal degradation, and recycling of some receptors (1), it may not be required for the normal trafficking of non-membrane-associated vesicle contents. Alternatively, internalization and transport of fluid phase markers may be mediated via a heterogenous population of nonacidic as well as acidic vesicles. The possible contribution of these or other mechanisms to the present observations will require further study.

APPENDIX

A. Models

Functions 2 and 3 are the solutions for any of the three minimal models shown below, where M represents extracellular medium, C_1 and C_2 are intracellular vesicular compartments, and C_1 and C_2 together represent total cell-associated inulin or $C(t)$. Models II and III are analogous to models previously considered by others in which the intracellular compartments C_1 and C_2 act in series or in parallel, respectively (6).

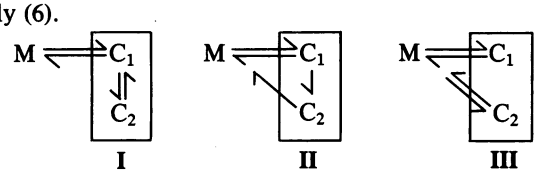

In the case of Models I and II, the function parameters have no simple interpretation. For Model III, P_1 is the pool size of the faster compartment characterized by the shorter half-life ln $2/P_2$, and P_3' is the pool size of the slower compartment characterized by the longer half-life ln $2/Q_4$. This model is selected for discussion purposes.

B. Integration of Data from Cultured Cells and Perfused Rat Liver

If

A = cold-sensitive rate of initial inulin uptake by cultured hepatocytes ($P_1 \cdot P_2 + P_3$; Function 1) = 0.0328 $\mu l \cdot mg^{-1} \cdot min^{-1}$,

B = cold-sensitive rate of net inulin accumulation in cultured hepatocytes (P_3; Function 1) = 0.0059 $\mu l \cdot mg^{-1} \cdot min^{-1}$ or

= net accumulation by perfused liver = 0.0048 $\mu l \cdot mg^{-1} \cdot min^{-1}$, and

C = rate of biliary inulin clearance (5) = 0.0006 $\mu l \cdot mg^{-1} \cdot min^{-1}$,

then, of total inulin taken up,

the fraction regurgitated = $[A - (B + C)]/A \simeq 0.80$,

the fraction sequestered = $B/A \simeq 0.18$, and

the fraction secreted in bile = $C/A \simeq 0.02$.

We thank Michael A. Wong for technical assistance. This work was supported in part by National Institutes of Health Grants AM-26270, AM-07453, AM-01254, and University of California, San Francisco, Liver Core Center Grant AM-26743 (including the Cell Culture, Perfused Liver, Microscopy, Biomathematics, and Editorial Core Facilities), as well as grants from the American Liver Foundation; The Walter C. Pew Fund for Gastrointestinal Research; the University of California, San Francisco, Committee on Research Evaluation and Allocation; and a fellowship from the Swiss National Science Foundation (E.L.R.).

1. Wileman, T., Harding, C. & Stahl, P. (1985) *Biochem. J.* **232,** 1–14.
2. Goldman, I. S., Jones, A. L., Hradek, G. T. & Huling, S. (1983) *Gastroenterology* **85,** 130–140.
3. Munniksma, J., Noteborn, M., Koorsha, T., Stienstra, S., Bouma, J. M. W., Gruber, M., Brouwer, A., Praaning-Van Duten, D. & Knook, D. L. (1980) *Biochem. J.* **192,** 613–621.
4. Ose, L., Ose, T., Reinertson, R. & Berg, T. (1980) *Exp. Cell Res.* **126,** 109–119.
5. Lake, J. R., Licko, V., Van Dyke, R. W. & Scharschmidt, B. F. (1985) *J. Clin. Invest.* **76,** 676–684.
6. Besterman, J. M., Airhart, J. A., Woodworth, R. C. & Low, R. B. (1981) *J. Cell Biol.* **91,** 716–727.
7. Morrill, G. A., Kostellow, A. B. & Weinstein, S. P. (1984) *Biochim. Biophys. Acta* **803,** 71–77.
8. van Deurs, B., Ropke, C. & Thorball, N. (1984) *Eur. J. Cell Biol.* **34,** 96–102.
9. Scharschmidt, B. F. & Stevens, J. E. (1981) *Proc. Natl. Acad. Sci. USA* **78,** 1321–1326.
10. Van Dyke, R. W. & Scharschmidt, B. F. (1983) *J. Biol. Chem.* **258,** 12912–12919.
11. Bissell, D. M. & Guzelian, P. S. (1980) *Ann. N.Y. Acad. Sci.* **349,** 85–89.
12. Meier, P. J., Sztul, E. S., Reubin, A. & Boyer, J. L. (1984) *J. Cell Biol.* **98,** 991–1000.
13. Lake, J. R., Van Dyke, R. W. & Scharschmidt, B. F. (1987) *Gastroenterology*, in press.
14. Lake, J., George, P., Licko, V. & Scharschmidt, B. F. (1985) *Clin. Res.* **33,** 322 (abstr.).
15. Lowe, P. J., Barnwell, S. G., Sharma, R. K. & Coleman, K. (1985) *Biochem. J.* **229,** 529–537.
16. Steinman, R. M., Mellman, I. S., Muller, W. A. & Cohn, Z. A. (1983) *J. Cell Biol.* **96,** 1–27.
17. Marshall, S. (1985) *J. Biol. Chem.* **260,** 13524–13531.
18. Steinman, R. M., Brodie, S. E. & Cohn, Z. A. (1976) *J. Cell Biol.* **68,** 665–687.
19. Spady, D. K., Turley, S. D. & Dietschy, J. M. (1985) *J. Clin. Invest.* **76,** 1113–1122.
20. Graf, J., Gautam, A. & Boyer, J. L. (1984) *Proc. Natl. Acad. Sci. USA* **81,** 6516–6520.
21. Schiff, J., Fisher, M. M. & Underdown, B. J. (1984) *J. Cell Biol.* **98,** 79–89.
22. Van Dyke, R. W., Steer, C. J. & Scharschmidt, B. F. (1984) *Proc. Natl. Acad. Sci. USA* **81,** 3108–3112.